Influence of Battery Models on the Optimal Design of the Propulsion System of a Hyperloop Capsule

Denis Tudor and Mario Paolone
École Polytechnique Fédérale de Lausanne

Abstract—The paper assesses the influence of equivalent circuit battery models on the optimal design of the propulsion system of an energy-autonomous Hyperloop capsule. By knowing a pre-determined payload to be transported along pre-determined trajectories, the problem minimizes the total number of battery cells supplying the capsule propulsion along with the maximization of its performance. The constraints of the problem embed numerically-tractable models of the main components of the electrical propulsion systems and of the battery. Although the optimization problem is non-convex, its constraints are formulated to exhibit a good numerical tractability. After having determined the solutions influenced by a weighting factor with two different battery models, dominant solutions are identified using specific metrics with the purpose of assessing the impact of the battery model on the determined solutions.

Nomenclature

Δx	Sampling distance interval of the capsule's trajectory
η	Efficiency of the capsule propulsion system (joint mechanical and electrical)
ρ	Hyperloop tube air density
A	Cross section surface of the capsule
a	Capsule's acceleration
C_d	Capsule drag coefficient
C_p	Capacitance of the 'p' RC branch of the cell Model 2 (TTC Model)
C_{batt}	Capacity of the battery for both cell models
F_{drag}	Capsule drag force
$F_{traction}$	Capsule traction force
L	Total length of the capsule trajectory
I_{batt}	Battery current for both cell models
I_{cell}	Cell current
k_1	Weight per unit power density of a linear induction motor
k_2	Weight per unit power density of a power electronic converter
L	Total length of the capsule trajectory
m	Total mass of the capsule
m_0	Passive mass of the capsule
m_{active}	Active mass of the capsule
m_{BESS}	Mass of the battery of the capsule
m_{cell}	Mass of a battery cell
$m_{mechanics}$	Mechanical mass of the capsule
$m_{payload}$	Payload mass of the capsule
m_{PS}	Mass of the capsule propulsion systems
n	Number of trajectory zones
N_p	Number of cells in parallel in the battery pack
N_s	Number of cells in series in the battery pack
P'_{batt}	Accessible power of the battery at its terminals for cell model 2
P_{batt}	Accessible power of the battery at its terminals for cell model 1
$P_{maxCell}$	Maximum power provided by a battery cell
P_{max}	Maximum electrical power of the capsule propulsion
$P_{traction}$	Capsule traction power
R_0	Equivalent series resistance of a battery cell for cell Model 2
R_{batt}	Equivalent series resistance of the battery for cell Model 1
R_{cell}	Equivalent series resistance of a battery cell for cell Model 1
R_p	Equivalent resistance of the 'p' RC branch of the cell Model 2 (TTC Model)
SoC	Battery state-of-charge for both cell models
SoC_{final}	Battery state-of-charge at the end of the capsule trajectory for both cell models
U_b	Accessible voltage of the cell at its terminals for cell Model 2
U_{C_p}	Voltage of the 'p' RC branch of the cell Model 2 (TTC Model)
v	Capsule's speed
V'_{batt}	Accessible voltage of the battery at its terminals for cell Model 2
V_{batt}	Accessible voltage of the battery at its terminals for cell Model 1
V_{cell}	Accessible voltage of the cell at its terminals for cell Model 1
V_{OCV}^{batt}	Open circuit voltage of the battery for both cell models
V_{OCV}^{cell}	Open circuit voltage of the cell for both cell models
w	Normalization factor in the objective function of the proposed optimization problem
x	Index of space associated to the position of the capsule along the trajectory

I. Introduction

One of the fundamental aspects in the design of a hyperloop transportation system lies in the optimal assessment of the energy reservoir that capsules need to carry along with the characteristics of its propulsion system (PS). Indeed, Hyperloop capsules are requested to be energy autonomous

vehicles in order to avoid the electrification of the vacuum tube where they are expected to travel at high speed. More specifically, Hyperloop capsules move into sealed and pre-determined trajectories confined by low-pressure operated tubes. The pressure inside the tube is pumped down to values of 5-10% (50-100mbar, e.g., [1]) of normal atmosphere, a condition that reduces the drag forces and increases the efficiency of this transportation system.

Concerning the specific problem of the optimal sizing of the PS and the battery energy storage system (BESS) of a Hyperloop capsule, it is a non-trivial one representing the main topic of this paper. A general optimization framework that leverages numerically-tractable models of the capsule PS, BESS and kinematics, is first presented. Then, a specific analysis of the influence of equivalent circuit battery models on the optimal design of the capsule's PS is given.

II. PROBLEM STATEMENT

A. Environment Conditions

As aforementioned, the closed and sealed trajectory of a Hyperloop allows pumping down the pressure to values in order of 5% (50mbar) of normal atmosphere. The total length of the trajectory is L and it is splitted into n different sections: $\{i_1, i_2, ..., i_n\}$ where x represents the generic position of the capsule (see Fig. 1).
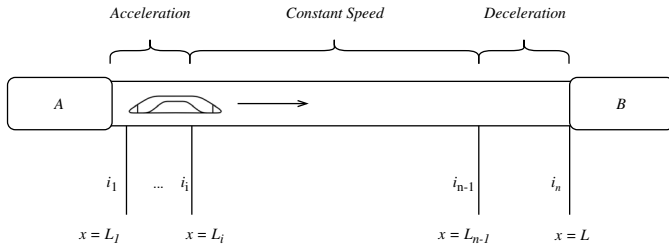

Fig. 1. The generic trajectory of Hyperloop.

The trajectory is then separated into acceleration, constant speed and deceleration zones (see Fig. 1). At the end of the acceleration zone, the capsule achieves the maximum allowable speed while, at the end of the constant speed zone, the capsule starts the braking to stop at $x = L$.

B. Propulsion System of the Capsule

The structure of the capsule's PS is supposed to be composed by three main sub-systems: (i) an energy reservoir represented by a BESS, (ii) a DC/AC converter and (iii) an electrical machine (e.g., a linear induction motor). In the following subsections, the main components are independently treated in order to formulate the targeted optimization problem.

1) Capsule's power source: the capsule's source of power is assumed to be a BESS. This specific component is here analyzed at the cell level concerning its modeling. As known, there are three main families of battery models [2], [3]: (i) the "bucket" models where cells are represented as integral operators of current/power with state variables being charge/energy; (ii) equivalent circuit models where the voltage dynamics

are simulated by means of an equivalent network of electric lumped components and the state-of-charge (SoC) is still modeled via an integral operator; (iii) electrochemical models where the cell internal dynamics associated to ion species diffusion and electrochemical reactions are fully modeled. In this work we adopted cell models belonging to the second above listed families. This choice has been preferred since it allows to derive a set of numerically tractable constraints capable to capture the main cell's response. Fig. 2 presents the simplest equivalent circuit of a cell (*cell Model 1*). Here below the description of the cell's quantities is given.

- V_{OCV}^{cell}: represents the open circuit voltage of the cell and it varies with SoC.
- I_{cell}: represents the current flowing in a single cell.
- R_{cell}: represents the equivalent series resistance (ESR) of the cell and the equivalent resistance of the cell's terminals connections with the next cell.
- V_{cell}: corresponds to the voltage accessible in correspondence of the cell's terminals; it is affected by the voltage drop produced by the R_{cell}.
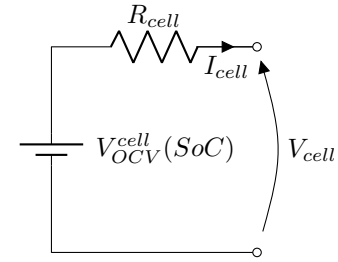

Fig. 2. Cell Model 1: first equivalent circuit of a cell adopted to derive the BESS constraints.

In a first approximation, the model of an entire BESS pack composed by identical cells can mathematically be described by (1), where N_s and N_p represent the number of series cells, respectively the parallel cells of the BESS, V_{OCV}^{batt} represents the open circuit voltage, which is solely a function of the cells SoC, while R_{batt} integrates the all the cells and connectors resistances. C_{batt} represents the capacity of the BESS. I_{batt} is the total current provided (or absorbed) by the BESS.

$$\begin{cases} V_{OCV}^{batt} = f(SoC) \\ V_{OCV}^{batt} = V_{OCV}^{cell} N_S \\ R_{batt} = R_{cell} \frac{N_s}{N_p} \\ I_{batt} = I_{cell} N_p \\ SoC = SoC(0) + \int_0^t \frac{I_{batt}}{C_{batt}} dt \end{cases} \quad (1)$$

Hence, V_{batt} and P_{batt}, are the accessible voltage and power of the BESS (2) for *cell Model 1*.

$$\begin{cases} V_{batt} = N_s(V_{OCV}^{cell} - R_{cell} I_{cell}) \\ P_{batt} = I_{batt} V_{batt} \end{cases} \quad (2)$$

The function $V_{OCV}^{batt}(SoC)$ is usually made available by the cells manufacturers.

The second model (*cell Model 2*) of the battery cell is the well-known two time constant (TTC) model capable to capture the charging/discharging and redistribution phases.

The equivalent circuit of the TTC model is shown in Fig. 3 and its mathematical model in the state space form in (3) (e.g., [4]).
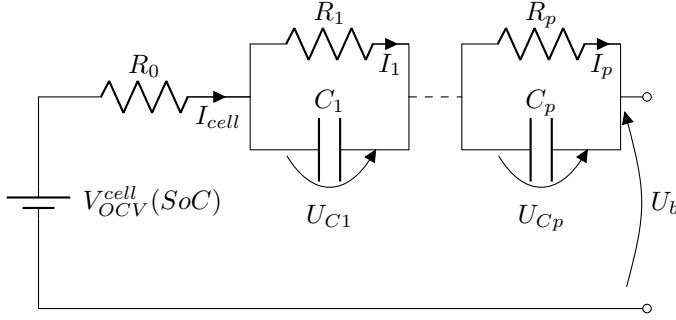

Fig. 3. Cell Model 2: second equivalent circuit of a cell used to derive the BESS constraints (in general, the TTC model can contain multiple RC series branches in order to improve its capability to model the charge diffusion).

$$\begin{bmatrix} \dot{U}_{C_1} \\ \dot{U}_{C_2} \\ . \\ . \\ \dot{U}_{C_p} \end{bmatrix} = \begin{bmatrix} \frac{1}{R_1 C_1} & 0 & ... & 0 \\ 0 & \frac{1}{R_2 C_2} & ... & 0 \\ 0 & ... & ... & 0 \\ 0 & 0 & ... & \frac{1}{R_p C_p} \end{bmatrix} \cdot \begin{bmatrix} U_{C_1} \\ U_{C_2} \\ . \\ . \\ U_{C_p} \end{bmatrix} + \begin{bmatrix} \frac{1}{C_1} \\ \frac{1}{C_2} \\ ... \\ \frac{1}{C_p} \end{bmatrix} \cdot I_{cell} \tag{3}$$

where:

- $U_{C_1}, U_{C_2}, ..., U_{C_p}$ are the voltages of the RC series branches;
- $C_1, C_2, ..., C_p$ are the capacitors of the RC branches;
- I_{cell} is the current flowing through the cell;
- R_0 is the ESR of the cell and cell's terminals connections.

The cell accessible voltage provided by the TTC model, U_b, is given by (4).

$$U_b = V_{OCV}^{cell}(SoC) - R_0 I_{cell} - U_{C_1} - U_{C_2}... - U_{C_p} \tag{4}$$

In the second approximation, the model of an entire BESS pack composed by identical cells can mathematically be described by (5).

$$\begin{cases} V_{OCV}^{batt} = f(SoC) \\ V_{OCV}^{batt} = V_{OCV}^{cell} N_S \\ I_{batt} = I_{cell} N_p \\ SoC = SoC(0) + \int_0^t \frac{I_{batt}}{C_{batt}} dt \end{cases} \tag{5}$$

Hence, V'_{batt} and P'_{batt}, are the accessible voltage and power of the BESS (6) for *cell Model 2*.

$$\begin{cases} V'_{batt} = N_s(V_{OCV}^{cell}(SoC) - R_0 I_{cell} - U_{C_1} - U_{C_2}... - U_{C_p}) \\ P'_{batt} = I_{batt} V'_{batt} \end{cases} \tag{6}$$

2) Propulsion: Speed and acceleration profiles are function of the traction force provided by different types of electrical motors characterized by different performance. For the motor and converter, the most important parameters are:

- $\frac{P}{weight}$ which represents the ratio between the total amount of power per unit mass of both DC/AC converter and the electrical machine.
- V_{DC}^{max} which represents the maximum allowable DC voltage of the DC/AC converter.

C. Capsule's Kinematic Model

The total mass of the system can be expressed as in (7) where m_0 represents the mass of the payload, $m_{payload}$, and the mechanical sub-systems masses, $m_{mechanics}$, such as the capsule aeroshell, chassis, pressure vessels, stability and braking mechanisms, electromagnets for the levitation sub-system, m_{BESS} represents the mass of the BESS while m_{PS} represents the mass of the propulsion system.

$$m = m_0 + m_{BESS} + m_{PS} \tag{7}$$

In what follows, we specifically refer to a PS composed by a linear induction motor (LIM) and a DC/AC converter (VSI). Therefore, the sub-system masses can be expressed in (9), where k_1 represents the weight per unit power density of a LIM and k_2 the weight per unit power density of a VSI. m_{cell} is the cell unitary mass and P_{max} represents the maximum instantaneous power of the capsule along the trajectory.

The definitions for k_1 and k_2 are given in (8), where m_{LIM} and m_{VSI} represent the mass for a LIM, respectively for a VSI, relative to the maximum power to be delivered along the trajectory for the LIM, P_{LIM}, and for the VSI, P_{VSI}.

$$k_1 = \frac{m_{LIM}}{P_{LIM}}; k_2 = \frac{m_{VSI}}{P_{VSI}} \tag{8}$$

$$\begin{cases} m_0 = m_{payload} + m_{mechanics} \\ m_{BESS} = N_s N_p m_{cell} \\ m_{PS} = P_{max}(k_1 + k_2) \end{cases} \tag{9}$$

In order to translate the mass of the PS as a function of the mechanical power of the capsule's PS, it is assumed that the maximum provided power by the BESS is equal to the maximum power of the LIM and of the VSI. Therefore, considering the global efficiency of the capsule PS, η, and the maximum deliverable power of a cell, $P_{maxCell}$, the total mass of the capsule can be expressed as in (10). Clearly, the possibility to correctly express $P_{maxCell}$ is function of the BESS model.

$$m = m_0 + N_s N_p m_{cell} + \frac{1}{\eta} P_{maxCell} N_s N_p (k_1 + k_2) \tag{10}$$

Along the trajectory, the acceleration, a, and the speed, v, are sampled at regular intervals, Δx, therefore, the total number of discrete analysis points is $[\frac{L}{\Delta x}]$.

The reduced drag force [5] of the Hyperloop system represents one of the most significant gains from the efficiency point of view since it is proportional to the tube's interior fluid density (ρ). The drag force is defined in (11), where C_d represents the drag coefficient of the capsule and A the cross section of the capsule.

$$F_{drag}(x) = \frac{1}{2} A C_d \rho v^2(x) \tag{11}$$

Given a and v along the trajectory, the propulsion system traction force and traction power are given by (12).

$$\begin{cases} F_{traction}(x) = ma(x) + F_{drag}(x) \\ P_{traction}(x) = F_{traction}(x) \cdot v(x) \end{cases} \tag{12}$$

By considering (10), (11) and (12), the traction power is represented by (13) as a function of m, a and v. The conclusion of (13) is that $P_{traction} \sim f(a; N_s N_p)$.

$$P_{traction}(x) = (ma(x) + F_{drag}(x)) \cdot v(x) \quad (13)$$

Once reaching the maximum speed, v_{max}, the instantaneous power consumption of the capsule is minimal due to (12). This simple observation, supported by the numerical results of section III, allows to state that the Hyperloop propulsion system application is closer to a power-intensive application rather than an energy-intensive one.

D. Formulation of the Optimization Problem

In the view of the various models of the components of the capsule's PS, we propose to formulate the problem for the optimal design of the PS as in (14) (independently with *cell Model 1* and *cell Model 2*).

The objective function is given by two factors: the number of BESS cells in the system and the performances of the capsule represented by the norm-2 of the array of the discrete accelerations sampled along the capsule's trajectory.

$$\min_{N_s N_p, a} \quad N_s N_p - w \cdot ||a(x)||_2$$

$$\text{subject to} \quad x \in [1, \frac{L_{n-1}}{\Delta x}]$$

$$v(x) \leq v_{max}$$

$$a_{min_1} \leq a_{i_1}(x) \leq a_{max_1}, \forall x \in [1; \frac{L_1}{\Delta x})$$

$$a_{min_2} \leq a_{i_2}(x) \leq a_{max_2}, \forall x \in [\frac{L_1}{\Delta x}; \frac{L_2}{\Delta x})$$

$$...$$

$$a_{min_{n-1}} \leq a_{i_{n-1}}(x) \leq a_{max_{n-1}},$$

$$\forall x \in [\frac{L_{n-2}}{\Delta x}; \frac{L_{n-1}}{\Delta x}]$$

$$\frac{L^2}{\sum_{x=1}^{\frac{L}{\Delta x}} v(x) \cdot \Delta x} \leq T_{max}$$

$$SoC_{max} \geq SoC \geq SoC_{min}$$

$$V_{OCV}^{cell}(0) = V_{OCV}^{cell}|_{SoC=SoC_{max}}$$

$$I_{cell}(x) \leq I_{cellMax}$$

cell Model 1 :		cell Model 2 :
$(1), (2)$		$(3), (4), (5), (6)$
$P_{traction} \leq \eta P_{batt}$	or	$P_{traction} \leq \eta P'_{batt}$

$$(7), (8), (9), (10), (11)$$

$$(14)$$

For the acceleration and constant speed zones, we know that $\frac{dv}{dx} \geq 0$. Therefore, we can say that:

$$min(\frac{L^2}{\sum_{x=1}^{\frac{L}{\Delta x}} v(x) \cdot \Delta x}) \iff max(v_{max}). \quad (15)$$

Since v_{max} can be expressed as:

$$v_{max} = \int_{x_0}^{x} a(\tau)d\tau \simeq \sum_{x_0}^{\frac{L_3}{\Delta x}} a(x)\Delta t, \quad (16)$$

From (15) and (16), if we want to maximize v_{max}, we have to maximize $\sum_{x_0}^{\frac{L_3}{\Delta x}} a(x)\Delta t$ which implies to maximize $|a(x)|_1$. We choose to maximize the $||a(x)||_2$ in order to give more weight to the higher values of the acceleration along the trajectory.

The $N_s N_p$ and $||a(x)||_2$ in (14) are represented by inhomogeneous physical quantities, therefore, a weight factor, w, is needed in order to normalize them. The maximum speed of the capsule cannot be larger than a pre-determined value, v_{max}, and the average journey time cannot pass a certain given threshold, T_{max}. Furthermore, the acceleration along the trajectory on i_1, i_2,..., i_{n-1} zones are bounded due to the human body limitations or expected performances. We have also constrained the I_{cell} to be lower than the maximum admissible discharge rate of the cell given by a certain technology. At the BESS layer, the V_{OCV}^{batt} is chosen with respect to the railway electrification system standard and the SoC should be in the safe range of functioning, bounded by SoC_{min} and SoC_{max}.

The deceleration performed on i_n (where the capsule activates the braking system) is supposed to have a dominant part of the braking force provided by a dissipative braking mechanism while a minimal part is provided by the regenerative one. Since the regenerative braking allows to recover a minimal part of the capsule's kinetic energy, it is not considered in the optimization problem. So, we assume to charge the BESS in the zone i_n with the maximum charging rate allowed by the BESS cells, $I_{cellMax_{charge}}$. This allows to compute the SoC at the end of the trajectory, SoC_{final}.

It is worth observing that the problem (14) is non-convex due to several of its constraints and it has been solved using a gradient-based method since both the objective function and constraints are continuous and have continuous first derivatives.

III. NUMERICAL ASSUMPTIONS AND RESULTS

A. Assumptions on the Capsule Trajectory

In order to present a numerical example, (14) is applied for a route in Switzerland between Geneva and Zürich. The length of the trajectory is $L = 226km$. The considered trajectory has been segmented in the zones reported in (17), where i_1 and i_2 represent the acceleration zones, while i_3 is the constant speed zone and i_4 the deceleration one. The discrete sampling of the trajectory is $\Delta x = 100m$, resulting in a total number of 2260 discrete points throughout the total space budget of the trajectory.

$$\begin{cases} i_1, \forall x \in [1; \frac{L_1}{\Delta x}), L_1 = 5km \\ i_2, \forall x \in [\frac{L_1}{\Delta x}; \frac{L_2}{\Delta x}), L_2 = 26km \\ i_3, \forall x \in [\frac{L_2}{\Delta x}; \frac{L_3}{\Delta x}), L_3 = 206km \\ i_4, \forall x \in [\frac{L_3}{\Delta x}; \frac{L}{\Delta x}), L = 226km \end{cases} \quad (17)$$

B. Assumptions on the Capsule and Propulsion System

The capsule is expected to be able to transport 25 people (the payload could be replaced by a cargo one). The average mass payload for a person is 80kg which represents $m_{payload} = 2000kg$.

1) Other general mechanical parameters: We assume $m_{mechanics} = 6000kg$, therefore $m_0 = 8000kg$, a frontal cross section surface $A = 6m^2$ [6] and the value of the drag coefficient $C_d = 0.1$ [7]. The aggregated efficiency of the LIM and VSI is also assumed to be $\eta = 0.95$. The acceleration boundaries are chosen to be in the same order of magnitude of maximum accelerations offered by modern passenger aircrafts in (18) where $g = 9.81\frac{m}{s^2}$.

$$\begin{cases} v_{max} = 1200\frac{km}{h} \\ T_{max} = 20min \\ a_{min_1} = 0.05g; a_{max_1} = 0.9g \\ a_{min_2} = 0.05g; a_{max_2} = 0.6g \\ a_{min_3} = 0g; a_{max_3} = 0.001g \end{cases} \quad (18)$$

2) BESS: Due to the high discharge rate, the chosen cell is the Kokam SLPB 11543140H5. It can sustain a continuous discharge rate up to $30C$. Its parameters have been fully-characterized at the Authors' laboratory. Regarding the maximum value of V_{OCV}^{batt} this is chosen based on [8], therefore $V_{OCV}^{batt} = 1.5kV$ for $SoC_{max} = 100\%$. The other limits are given in (19). For the TTC model (*cell Model 2*), two RC branches have been chosen additionally to the ESR as shown in Fig. 4.

$$\begin{cases} SoC_{max} = 100\% \\ SoC_{min} = 10\% \\ R_{cell} = R_0 = 4.4m\Omega \\ R_1 = 12.2m\Omega \\ C_1 = 7380.96F \\ R_2 = 1.3m\Omega \\ C_2 = 2370.78F \\ m_{cell} = 0.128kg \\ I_{cellMax} = 150A \\ I_{cellMax_{charge}} = 5A \end{cases} \quad (19)$$
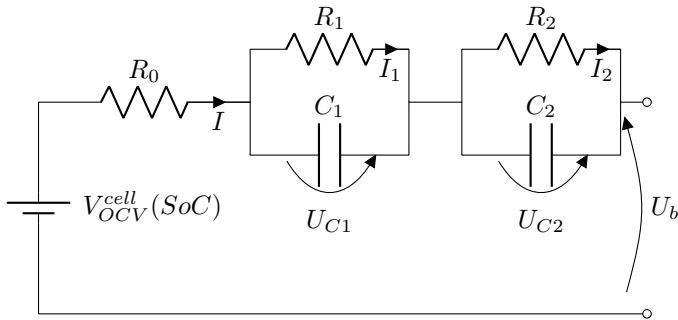
Fig. 4. Cell Model 2: second equivalent circuit of a cell adopted to derive the BESS constraints.

3) Propulsion: The weight per unit power density of the LIM, k_1, is selected by making reference to a Hyperloop prototype developed at the Authors laboratory whilst the same parameter for the VSI, k_2, has been inferred using industrial-grade VSI used in the automotive sector (Brusa Motors).

$$k_1 = 0.091\frac{kg}{kW}; k_2 = 0.075\frac{kg}{kW} \quad (20)$$

C. Results

The problem (14) was solved using the Algorithm 1 where the weight parameter, w, has been varied and the control variables $N_s N_p$ and a have been initialized with different values in a range of having a feasible technical meaning. The problem independently addressed the two considered cell models (Model 1 and Model 2) and generated different results. By using Algorithm 1, the following figures represent the two different fronts corresponding to the *cell Model 1* and *cell Model 2* of BESS as a function of w (for each w, the obtained solutions represent the best minimum for (14) given by the several initialization). Fig. 5 shows the capsule and BESS masses, Fig. 6 and Fig. 7 the maximum speeds and accelerations achieved along the trajectory, Fig. 8 the maximum traction powers and Fig. 9 the average times necessary to cover the trajectory with the two different cell models.

Algorithm 1

1: **for** $w = 10^0 \rightarrow 10^8$
2:   **for** $a_{init} = 0 \rightarrow 1, \Delta a_{init} = 0.1$
3:     **for** $N_s N_{p,init} = 0 \rightarrow 10000, \Delta N_s N_{p,init} = 1000$
4:       Solve (14)
5:     **end for**
6:   **end for**
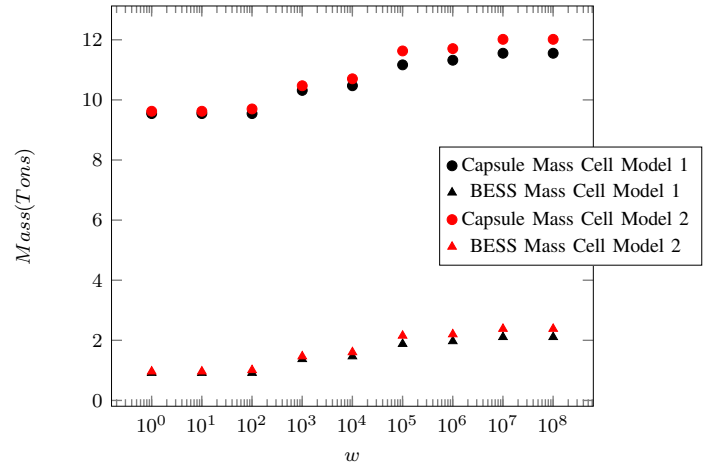7:   Find $N_s N_p$ and a with min obj
8: **end for**

Fig. 5. Capsule and BESS masses.

IV. DISCUSSIONS

A. General Observations

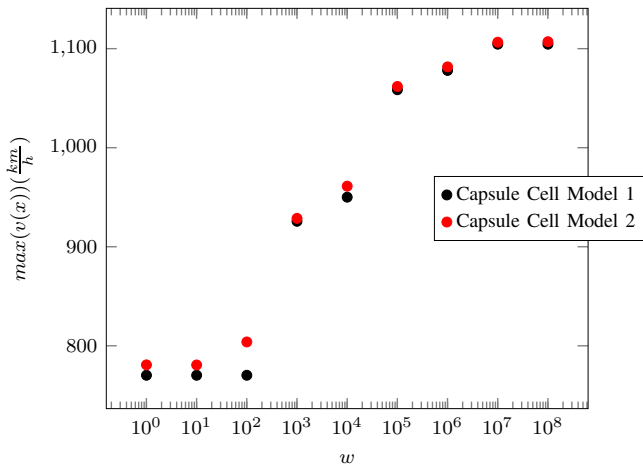Nine different capsule-PS solution spaces for every cell model were generated depending on the value of w. The
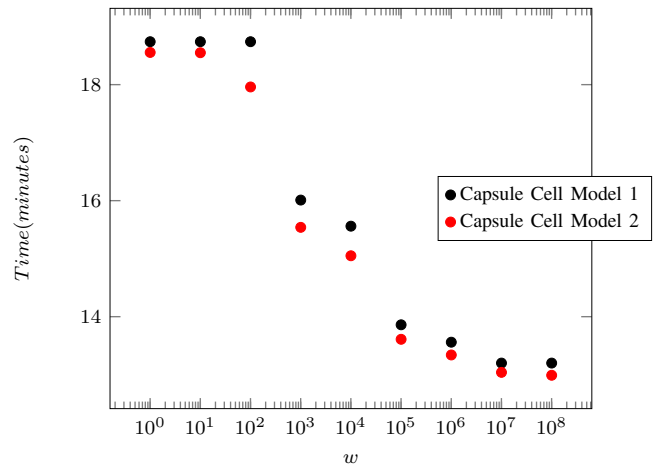
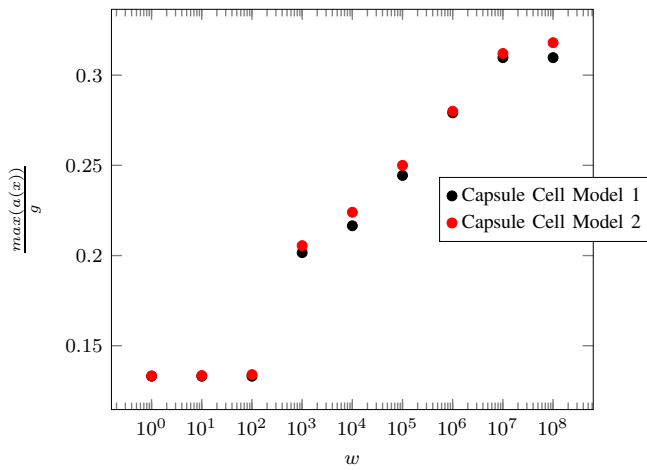Fig. 6. Maximum speed along the trajectory.

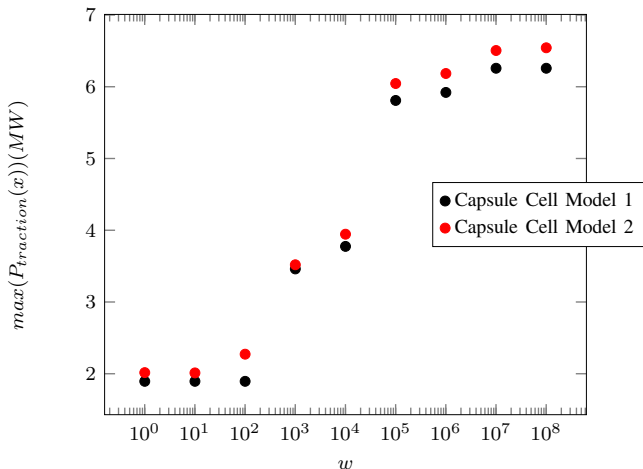Fig. 7. Maximum acceleration along the trajectory (values in per-unit to g).

Fig. 8. Maximum traction power provided by the capsule propulsion system.

nine solutions represent various trade-offs between the average traveling time and either energy consumption or maximum required instantaneous power.

Irrespectively of the value of w or the cell model, it is

Fig. 9. Time necessary to cover the trajectory.

important to observe that the obtained BESS masses and the total number of cells are compatible with the currently proposed applications in commercial heavy-duty electric ve-hicles (e.g., electric trucks). The same observation applies to the maximum powers obtained for the other elements of the capsule propulsion. Therefore, the results indicate the technical feasibility of the identified capsule propulsion using today's technologies.

Indeed, in a range of $[0.9, 2]tons$ for *cell Model 1* and $[0.95, 2.4]tons$ for *cell Model 2* of battery cells (Fig. 5), most of the mass is still distributed to the mechanical sub-systems and for the payload. The amount of maximum power necessary to transport a payload of 25 people is in the range of $[2, 6.5]MW$ for *cell Model 1* and in the range of $[2.1, 6.6]MW$ *cell Model 2*. In Fig. 9, the average traveling time stays in the range of $[13, 19]minutes$ for both cell models, where the upper boundary of this range is constrained by the optimization problem and is governed by the lower values of w ($w = \{1, 10, 100\}$). Indeed, the average traveling time (Fig. 9) is related to the maximum speed over the trajectory (see Fig. 6) and the acceleration profile, where every maximum point, with respect to w, can be found in Fig. 7.

As a final remark, it is worth computing the capsule's energy consumption/km/passenger. The results are shown in Fig. 10 and we have assumed a BESS charging efficiency $\eta_{charging} = 89.4\%$ [9]. This estimation refers to the both cell models and only to the energy consumption of the capsule and does not include any vacuuming process.

B. Dominant Solutions

The dominant solution for the capsule PS should be identi-fied by looking at solutions preserving capsule's performances. Hence the first metric to be used to identify a dominant solu-tion can be represented by: $O_1 = \frac{max(P_{traction})}{TravelTime}$. This quantity is minimal for $w = 1$, and the value of $O_1 = 0.101\frac{MW}{min}$.

The auxiliary quantity to identify a potential different dom-inant solution takes into account the energy consumption with respect to the travel time: $O_2 = \frac{Energy}{Distance \cdot Passenger \cdot TravelTime}$ which is also minimal for $w = 1$ (with $O_2 = 1.11\frac{Wh}{km \cdot passenger \cdot min}$).
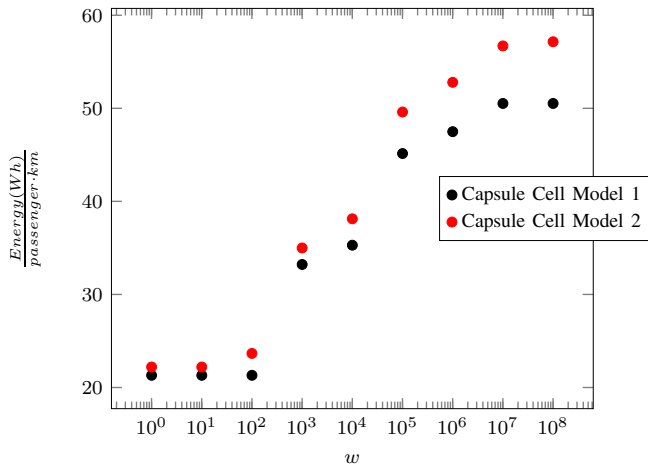
Fig. 10. The energy consumption per passenger per km.

Fig. 11. BESS relative difference depending on the battery cell model.

The optimal values, O_1 and O_2, regard the *cell Model 1*. The analogy for the *cell Model 2*, which eventually creates O'_1 and O'_2, coincides with the same w value ($w = 1$). Therefore, for both cell models, the dominant solutions could be found at $w = 1$.

C. Influence of cell models

The Algorithm 1 was applied for both aforementioned cell models. The TTC model (*cell Model 2*) generally restricts the sizing of the BESS to higher values of the energy-reservoir *cell Model 1*. The additional weight of cells is in a range of $[4, 12.5]\%$ as shown in Fig. 11. The computation has been made for every w. Nevertheless, it is worth observing that the average time travel is slightly reduced. Along with the mass of the BESS associated to *cell Model 2*, the energy consumption/km/passenger is heightened with a maximum of 12.2% for higher values of w. For lower values of w, the differences between the energy consumption/km/passenger term are not relevant as the BESS masses do not exceed a 4% relative difference.

The impact of the TTC model (*cell Model 2*) is evident, and it independently results in a larger BESS mass. Larger BESS masses associated to the usage of *cell Model 2* were expected as this model results in larger losses and voltage variations compared to *cell Model 1*.

V. CONCLUSIONS

The study has proposed an optimization problem of the propulsion system for a Hyperloop capsule. A comprehensive analysis of the results is given for the different weights of the terms in the objective function. The analysis of the results demonstrates the technical feasibility of the Hyperloop PS, with respect to existing BESS (regarding the two different cell models) and electrical propulsion technologies. Furthermore, our solutions enable us to compute energy consumption of the capsule's propulsion for *cell Model 1* between 22 to 50 Wh/km/passenger and for *cell Model 2* between 22.2 to 57.15 Wh/km/passenger. With the proposed analysis, we conclude that today's b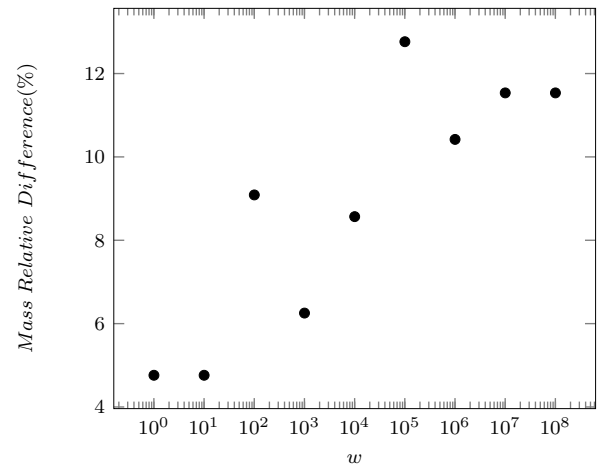attery and power-electronics technologies exhibit characteristics that are compatible with the Hyperloop application, thus enable its development as a viable transportation solution.

REFERENCES

[1] SpaceX, "SpaceX Hyperloop Pod Competition Rules," January 2016.
[2] S. Santhanagopalan, Q. Guo, P. Ramadass, and R. E. White. Review of models for predicting the cycling performance of lithiumion batteries. Journal of Power Sources, 156(2):620–628, 2006.
[3] M. R. Jongerden and B. R. Haverkort. Which battery model to use? IET software, 3(6):445–457, 2009.
[4] A. Rufer, "Energy Storage Systems and Components", Northwestern U.S.A.: CRC Press, Taylor and Francis Group, 2018, pp. 68-70.
[5] Liversage, P., and Trancossi, M., "Analysis of triangular sharkskin profiles according to second law," Modelling, Measurement and Control B. 87(3), 188-196, September 2018.
[6] Bombardier CRJ-1000 Aircraft, "CRJ Series," Technical Report, [online] https://commercialaircraft.bombardier.com/themes/bca/pdf/Bombardier_CRJ_Series_Brochure.pdf, 2017.
[7] Max M. J. Opgenoord and Philip C. Caplan, "Design of the Hyperloop Concept," AIAA Journal 2018 56:11, 4261-4270.
[8] "IEC 60850:2014 International Electrotechnical Commission–Railway applications - Supply voltages of traction systems," November 2014.
[9] J. Sears, D. Roberts and K. Glitman, "A comparison of electric vehicle Level 1 and Level 2 charging efficiency," 2014 IEEE Conference on Technologies for Sustainability (SusTech), Portland, OR, 2014, pp. 255-258.